



**HAL**  
open science

## Phosphanyl-substituted siloles: synthesis, optical and electrochemical studies and computations

Reka Mokrai, Tamás Holczbauer, Csaba Fekete, Balázs Volk, Vincent Dorcet, Pierre-Antoine Bouit, László Nyulászi, Muriel Hissler, Ilona Kovács, Zoltán Benkő

► **To cite this version:**

Reka Mokrai, Tamás Holczbauer, Csaba Fekete, Balázs Volk, Vincent Dorcet, et al.. Phosphanyl-substituted siloles: synthesis, optical and electrochemical studies and computations. *European Journal of Inorganic Chemistry*, 2020, 2020 (18), pp.1794-1802. 10.1002/ejic.202000163 . hal-02532057

**HAL Id: hal-02532057**

**<https://hal.science/hal-02532057>**

Submitted on 4 Apr 2020

**HAL** is a multi-disciplinary open access archive for the deposit and dissemination of scientific research documents, whether they are published or not. The documents may come from teaching and research institutions in France or abroad, or from public or private research centers.

L'archive ouverte pluridisciplinaire **HAL**, est destinée au dépôt et à la diffusion de documents scientifiques de niveau recherche, publiés ou non, émanant des établissements d'enseignement et de recherche français ou étrangers, des laboratoires publics ou privés.

# Phosphanyl-substituted siloles: synthesis, optical and electrochemical studies and computations

Réka Mokrai<sup>a,b</sup>, Tamás Holczbauer<sup>c</sup>, Csaba Fekete<sup>a,d</sup>, Balázs Volk<sup>e</sup>, Vincent Dorcet<sup>b</sup>, Pierre-Antoine Bouit<sup>b</sup>, László Nyulászi<sup>a,d</sup>, Muriel Hissler<sup>\*b</sup>, Ilona Kovács<sup>\*a</sup>, Zoltán Benkő<sup>\*a</sup>

- [a] R. Mokrai, Dr. Cs. Fekete, Prof. L. Nyulászi, Dr. I. Kovács, Dr. Z. Benkő  
Department of Inorganic and Analytical Chemistry, Budapest University of Technology and Economics  
Szt. Gellért tér 4, H-1111 Budapest, Hungary  
E-mail: ikovacs@mail.bme.hu  
E-mail: zbenko@mail.bme.hu
- [b] R. Mokrai, Dr. V. Dorcet, Dr. P-A. Bouit, Prof. M. Hissler  
Univ. Rennes, CNRS, ISCR - UMR 6226, F-35000 Rennes  
E-mail : muriel.hissler@univ-rennes1.fr
- [c] Dr. T. Holczbauer  
Research Centre for Natural Sciences, Institute of Organic Chemistry and Chemical Crystallography Research Laboratory  
Magyar Tudósok körútja 2, H-1117 Budapest, Hungary
- [d] Prof. L. Nyulászi  
MTA-BME Computation Driven Chemistry Research Group  
Szt. Gellért tér 4, H-1111 Budapest, Hungary
- [e] Dr. B. Volk  
Directorate of Drug Substance Development, Egis Pharmaceuticals Plc.  
P.O. Box 100, H-1475 Budapest, Hungary

## Abstract

In this paper, we report the synthesis and characterization of a series of phosphanyl-substituted siloles. The chemical modification (oxidation, sulfurization, alkylation and complexation) results in a change in the energy levels of frontier orbitals, which has further been studied by UV-Vis absorption spectroscopy and electrochemistry. Significantly, despite their high “s”

character the phosphorus lone pairs of the 2,5-bisphosphanylsilole can combine with the  $\pi$ -system of the silole core resulting in a somewhat destabilized HOMO. The structural aspects of these new siloles have been investigated employing single-crystal X-ray diffraction and DFT calculations.

## Introduction

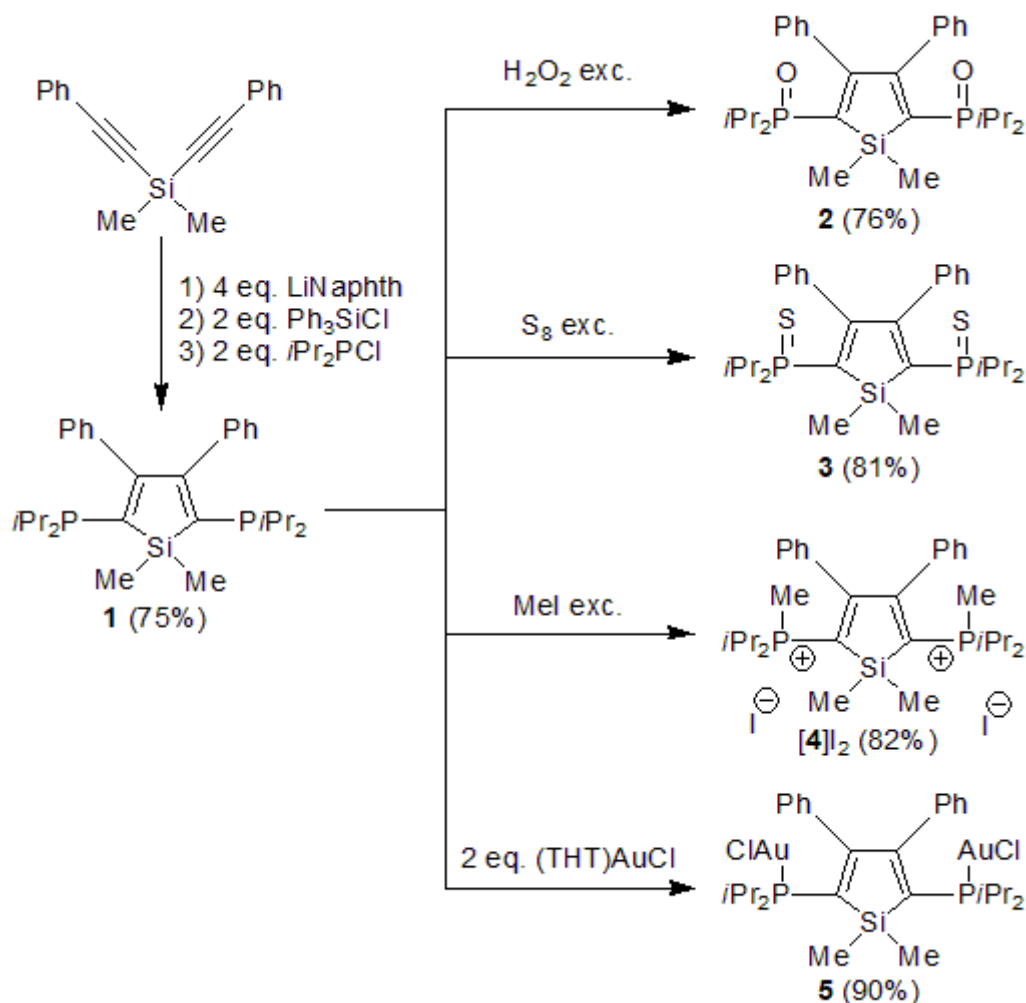
Due to their versatile electronic structures induced by the heteroatom, five-membered heterocycles have become useful synthons in optoelectronics.<sup>[1,2]</sup> *1H*-Siloles (silicon-containing heterocyclopentadienes) exhibit an unusually high electron affinity due to a hyperconjugative interaction between the  $\pi^*(b_1)$  orbital of the butadienic unit and the silyl  $\sigma^*(b_1)$  orbitals resulting in a significant stabilization of the silole LUMO.<sup>[3]</sup> Thus, the HOMO–LUMO gap of silole-containing  $\pi$ -conjugated systems is reduced compared to many other related  $\pi$ -conjugated systems, allowing for semiconductor application in electronic devices, such as organic light-emitting diodes (OLEDs), organic field-effect transistors (OFETs) or photovoltaic devices.<sup>[4–10]</sup> Even more interestingly, phenyl-substituted siloles may show aggregation-induced emission (AIE) enabling the synthesis of efficient emitters for OLEDs<sup>[11]</sup> or biosensors<sup>[12]</sup> exhibiting significantly stronger fluorescence in the solid-state than in solution. The optical properties of these molecules can be fine-tuned, for example, by changing the nature of the substituents at the five-membered ring. For example, electronegative substituents at the silicon center shift the UV-Vis absorption maxima to longer wavelengths,<sup>[14]</sup> while in the case of spiro compounds the UV-Vis absorption maxima are blue-shifted.<sup>[15]</sup> The substituents at the silicon center directly influence the above discussed hyperconjugative interaction, while the substituents at the 2 and 5 positions of the five-membered core may possess both  $\sigma$  and  $\pi$  donating/accepting properties, moreover, they can connect the silole ring with other conjugated systems allowing further fine-tuning of the optical and electrochemical properties of  $\pi$ -systems.<sup>[16–18]</sup>

Incorporation of phosphorus into  $\pi$ -conjugated systems and further post-functionalization at the P center is an efficient way to further tune the optical and redox properties.<sup>[19–21]</sup> In this context, we were interested in the introduction of P-atoms at the periphery of a silole ring. Although one diphenylphosphanyl-substituted silole and its P-oxidized analogue have been reported in the literature<sup>[22]</sup>, together with their UV-Vis absorption spectra, the effect of the phosphanyl substituents on the electronic properties has not been analyzed in detail. Here, we report the synthesis of a set of 2,5-bis(diisopropylphosphanyl)siloles together with their structural UV-Vis spectroscopic and cyclic voltammetric characterization, as well as computational studies

(conformations, analysis of molecular orbitals and TD-DFT calculations) to reveal the effects of the modification at the phosphorus center.

## Results and Discussion

### Synthesis



**Scheme 1:** Synthesis of phosphanyl-functionalized siloles **1–5** (Naphth: naphthalenide, THT: tetrahydrothiophene).

For the synthesis of diisopropylphosphanyl-substituted silacyclopentadienes (**Scheme 1**), we modified the reductive cyclization method described by Tamao and co-workers and Braddock-Wilking and co-workers.<sup>[22,23]</sup> To form the five-membered ring framework, 4 equivalents of lithium naphthalenide (LiNaphth) and dimethyl-bis(phenylethynyl)silane were reacted at –60°C, delivering the dilithio-substituted silole ring. To quench the excess of lithium naphthalenide, which is necessary for the efficient ring closure in reaction step 1, we used the

cheap chlorotriphenylsilane, instead of the reactant chlorodiisopropylphosphine, and subsequently, 2 equivalents of chlorodiisopropylphosphine were added to form the phosphanyl-substituted silole **1**. After crystallization, **1** was obtained as yellow, air-sensitive crystals in 75% yield. Various methods of P-functionalization were tested with compound **1** as starting material. The treatment of derivative **1** with an excess of 30% aqueous solution of H<sub>2</sub>O<sub>2</sub> resulted in the quantitative formation of phosphine oxide **2**, which was isolated *via* extraction (with dichloromethane as solvent) and crystallization as a white solid in 76% yield. Furthermore, the reaction of **1** with elemental sulfur in diethyl ether delivered compound **3**, which was isolated in 81% yield as a yellowish white solid. Dialkylation of **1** with an excess of methyl iodide in diethyl ether resulted in the formation of the bisphosphonium iodide [**4**]**I**<sub>2</sub>, isolated as a yellow solid in 82% yield. Moreover, we studied the complexation of silole **1**, which was reacted with chloro(tetrahydrothiophene)gold(I) [(THT)AuCl] in dichloromethane at room temperature to afford **5** as a white solid in 90% yield. While **1** is highly sensitive towards oxidation, compounds **2–5** are air- and moisture-stable powders. All of these compounds were characterized by multinuclear NMR and UV-Vis spectroscopy, high-resolution mass spectrometry, X-ray crystallography (except [**4**]**I**<sub>2</sub>) and elemental analysis.

### Heteronuclear NMR studies

In the <sup>31</sup>P{<sup>1</sup>H} NMR spectrum of silole **1**, the singlet resonance corresponding to the two equivalent P nuclei appears at  $\delta = +8.6$  ppm (**Table 1**), which is shifted downfield compared to the chemical shift of the 2,5-bis(diphenyl phosphanyl)-substituted silole ( $\delta$  <sup>31</sup>P{<sup>1</sup>H} =  $-12.2$  ppm<sup>[22]</sup>). This difference is primarily attributable to the different organic substituents at the P centers (note that the <sup>31</sup>P NMR chemical shift of P*i*Pr<sub>3</sub> and PPh<sub>3</sub> are  $+19.3$  and  $-5.2$  ppm, respectively).<sup>[24–26]</sup> The oxidation of **1** results in a downfield shift of  $\Delta\delta = \delta(\mathbf{2}) - \delta(\mathbf{1}) = +43.5$  ppm in the <sup>31</sup>P{<sup>1</sup>H} NMR spectra, which is comparable to that described earlier for P(O)*i*Pr<sub>3</sub> and P*i*Pr<sub>3</sub> ( $\Delta\delta = +35.7$  ppm).<sup>[27]</sup> When sulfur was applied as oxidant, again a downfield shift was observed, which is somewhat larger ( $\Delta\delta = \delta(\mathbf{3}) - \delta(\mathbf{1}) = +54.9$  ppm) compared to that for **2**. The smallest, but still significant downfield shift change of  $\Delta\delta = \delta([\mathbf{4}]\mathbf{I}_2) - \delta(\mathbf{1}) = +29.8$  ppm compared to **1** was obtained for compound [**4**]**I**<sub>2</sub>. The <sup>31</sup>P NMR chemical shift of complex **5**, in which each of the lone pairs of the two P atoms coordinates to gold(I) centers, is observed at  $+47.1$  ppm, which is somewhat larger than in case of the previously described digold complex of a bis(diphenylphosphanylphenyl)-substituted silole ( $\delta = +32$  ppm).<sup>[22]</sup> In summary, all the

chemical modifications of the P centers result in a substantial downfield shift compared to the chemical shift of  $\lambda^3$ -phosphanyl groups in silole **1**.

In the  $^{29}\text{Si}\{^1\text{H}\}$  NMR spectrum, the signal of **1** appears as a triplet at +12.6 ppm, showing the coupling of the  $^{29}\text{Si}$  nucleus with two magnetically equivalent phosphorus nuclei ( $^2J_{\text{P,Si}} = 8.5$  Hz). This chemical shift and  $^2J_{\text{P,Si}}$  coupling constant are comparable to the data reported for the bis(diphenylphosphanyl)-substituted silole (+15.1 ppm,  $^2J_{\text{P,Si}} = 8.5$  Hz).<sup>[22]</sup> Similarly, compounds **2–5** show triplet resonances in the  $^{29}\text{Si}\{^1\text{H}\}$  NMR spectra and all the chemical modifications (oxidation, sulfurization, alkylation, complexation) at the phosphorus centers lead to a downfield shift compared to silole **1** (Table 1). The changes in the  $^{29}\text{Si}\{^1\text{H}\}$  NMR spectra are in line with those observed in the  $^{31}\text{P}\{^1\text{H}\}$  NMR investigations, however, the changes are less pronounced. The  $^2J_{\text{P,Si}}$  coupling constants in compounds **1–5** are in the range of  $^3J_{\text{P,Si}}$  values reported for  $\beta$ -silyl phospholes (2–20 Hz).<sup>[28,29]</sup>  $^1\text{H}$  and  $^{13}\text{C}$  NMR resonances are observed in the typical regions reported for similar compounds.<sup>[22,23,30]</sup>

**Table 1.** Selected NMR data for compounds **1–5** (measured in  $\text{C}_6\text{D}_6$  for **1**,  $\text{CDCl}_3$  for **2–[4]I<sub>2</sub>** and  $\text{CD}_2\text{Cl}_2$  for **5**).

	$\delta$ $^{31}\text{P}\{^1\text{H}\}$ NMR (ppm)	$\delta$ $^{29}\text{Si}\{^1\text{H}\}$ NMR (ppm)	$^2J_{\text{P,Si}}$ (Hz)
<b>1</b>	+8.6	12.6	8.5
<b>2</b>	+52.1	23.1	10.5
<b>3</b>	+63.5	22.4	15.7
<b>[4]I<sub>2</sub></b>	+38.4	24.0	18.7
<b>5</b>	+47.1	18.4	17.6

### Structural studies

Compounds **1**, **2**, **3** and **5** were successfully crystallized and their molecular structures were determined by single crystal X-ray diffraction and the corresponding molecular structures are shown in **Figure 1**.<sup>[31]</sup>

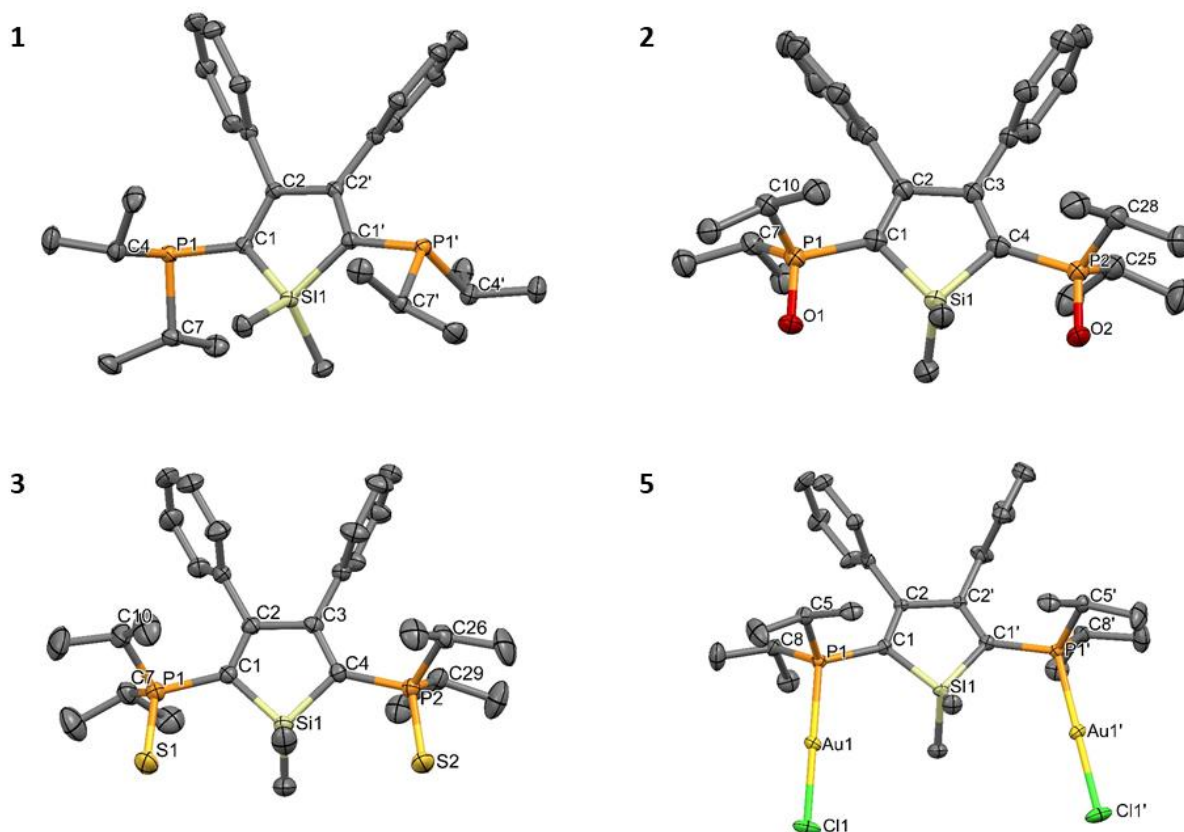


**Figure 1.** ORTEP representation of **1**, **2** and **5** at 50% probability level and **3** at 30% probability level (hydrogen atoms and solvent molecules are omitted for clarity). Selected bond lengths (in Å) and angles (°) of **1**: Si(1)–C(1) 1.885(1), C(1)–C(2) 1.362(1), C(2)–C(2') 1.518(2), C(1)–P(1) 1.830(1), C(1)–P(1)–C(4) 98.66(5), C(4)–P(1)–C(7) 102.75(5), C(1)–P(1)–C(7) 102.52(5). For compounds **2**, **3** and **5** see **Table S4**.

Compounds **1** and **2** crystallize in monoclinic crystal system with space group  $I2/a$  and  $P2_1/c$ , respectively. The asymmetric unit of **1** includes half molecule and a two-fold axis through the Si center can be found, while that of **2** contains one silole ring with three water molecules. The thiophosphoranyl-substituted silole **3** crystallizes in the monoclinic crystal system with space group  $P2_1/c$  and the asymmetric unit contains a whole molecule. Complex **5** crystallizes in the orthorhombic crystal system with space group  $Pnma$ , and due to the presence of a mirror

plane there is only half of the molecule and half of the dichloromethane solvent in the asymmetric unit.

In all the structures in **Figure 1**, the silicon resides in a tetrahedral coordination sphere. As expected, the three-coordinate phosphorus center of **1** is rather pyramidalized (sum of bond angles around phosphorus:  $\sim 304^\circ$ ), while the four-coordinate P centers in compounds **2**, **3** and **5** are in a distorted tetrahedral coordination environment.

The bond lengths in the silole core are similar to those previously described for silacyclopentadiene rings.<sup>[30,32]</sup> In each of the five-membered rings **1**, **2**, **3** and **5** the Si–C( $\alpha$ ) bond lengths are around 1.88 Å, a typical value for single bonds.<sup>[33]</sup> The C( $\alpha$ )–C( $\beta$ ) bond distances are significantly shorter than the ones between the C( $\beta$ ) and C( $\beta'$ ) centers (e. g. for **1** 1.362(1) Å vs. 1.518(2) Å), indicating that the bond between C( $\alpha$ ) and C( $\beta$ ) is basically a double-bond, while the C( $\beta$ )–C( $\beta'$ ) bond is practically a single bond. The NICS(0) values at the B3LYP/6-311+G\*\*//B3LYP/6-31+G\* level are in the range of –1.5 to +1.5 ppm for all the compounds showing minor variations, in accordance with the small effect of the P-substituent on the ring geometry. Altogether, the aromatic character of the silole ring is, as expected, very low, and a four-center delocalization is only observed in the  $\pi$  system involving the four carbon atoms, which is in a good agreement with the earlier description of 1,1-dimethyl-2,3,4,5-tetraphenylsilole.<sup>[34]</sup> The P–C( $\alpha$ ) distances are in the range of 1.79–1.83 Å, which is typical for P–C single bonds,<sup>[35]</sup> the longest distances were observed for **1**. The P=O distances in phosphine oxide **2** are 1.503(2) Å and 1.501(2) Å (cf. 1.48 Å in O=PPh<sub>3</sub>).<sup>[36]</sup> For **3**, the P–S distances are 1.953(1) and 1.954(1) Å, (cf. 1.954(1) Å in di(indenyl)phenyl phosphine sulfide).<sup>[37,38]</sup> In case of the gold complex **5**, the metals are coordinated in the usual linear arrangement to each phosphorus center (P–Au–Cl angle 179.62(5) °). The Au–P and Au–Cl bond lengths are 2.242(1) Å and 2.296(1) Å, respectively, which are comparable to those in

previously described compounds.<sup>[22,39,40]</sup> In the solid state, no short contacts characteristic for aurophilic interaction were observed between the gold centers.

It is noteworthy that while in **1** the *i*Pr groups point away from the phenyl substituents, for the rest of the compounds the substituents at the phosphino group are in-plane pointing away from the phenyl groups, in accordance with their steric need, which exceeds that of the lone pair of **1**. We studied the possibilities of different conformations for the parent compound **1** at the  $\omega$ B97XD/cc-pVDZ level and obtained several rotational isomers. The rotamers in which the P lone pairs point in the direction of the phenyl substituents (similarly to the X-ray structure) have rather similar energies (energy difference below 4 kcal/mol, see rotamers **1A–1H** in **Table S5**). In contrast the rotamer in which the P lone pairs are located in the other direction (**1I**) has a much higher energy (11.3 kcal/mol compared to the most stable rotamer **1A**), indicating a significant steric repulsion between the phenyl and the *i*Pr substituents in this arrangement. This is further demonstrated by the P–C( $\alpha$ )–C( $\beta$ ) angle, which is 121.84(8) $^\circ$  for **1**, and opens up to 131.1(2) $^\circ$  in case of **2**. This steric repulsion can also be observed in the dihedral angle of the phenyl rings, which are closer to perpendicular in **2**, **3** and **5** than in **1** (e. g. 73.8(4) $^\circ$  and 85.9(3) $^\circ$  in **2**, while 61.33(15) $^\circ$  in **1**). Accordingly, the P functionalized species (**2**, **3** and **5**) should be conformationally more rigid than **1**.

In order to understand the effect of the modification at the phosphorus centers in siloles **1–5**, we performed theoretical calculations, cyclic voltammetry measurements as well as UV-Vis absorption studies (see below). In the following the orbital energies obtained at the  $\omega$ B97XD/cc-pVDZ(PCM) level ( $\omega$ B97XD/cc-pVDZ(-PP)(PCM) level for the gold complex **5**) with dichloromethane as solvent are discussed – for more information on the computational method see the Supporting Information.

Frontier molecular orbitals, and electrochemical studies

The model 1,1,2,5-tetramethyl-3,4-diphenylsilole (**M**) is employed as a reference. As expected both HOMO and LUMO are  $\pi$  type orbitals at the silole core, with an energy gap of 8.20 eV. For the parent compound **1**, we also studied the effect of the above discussed various conformations, except the high energy **1H**. The LUMO of **1** is similar to that of **M** (**Figure 2**), and it is stabilized uniformly by 0.54 eV for all low-energy rotamers. The HOMO of **1** is, however, somewhat different from that of **M**, having additional contribution from the lone pairs of the two phosphorus. Importantly, the destabilization and the contribution of the lone pair differs somewhat for the rotamers. Although the overlap between the  $\pi$ -system and the phosphorus lone pair is limited by the significant “s” character of the latter, the energy difference between the  $\pi$ -orbital ( $\epsilon=-7.62$  eV for **M**) and the lone pair ( $\epsilon=-8.09$  eV for *iPr*<sub>2</sub>MeP) is small, thus their interaction is still non-negligible. Altogether, from the combination of the two phosphorus lone pairs and the silole  $\pi$  orbital three MOs arise, and the highest energy combination will be the HOMO. Depending on the orientation of the phosphanyl substituents two prototype situations were found as it is depicted for rotamers **1A** and **1B** in **Figure 3**, for the other isomers the situation is similar to either of these two rotamers. In one case (rotamer **1A**) only one of the two lone pairs at the phosphanyl centers contributes to the HOMO, and the HOMO-1 is basically the other lone pair, while the HOMO-3 is a symmetric combination of the  $\pi$  system and the two lone pairs. In the other case (the *C*<sub>2</sub> symmetric rotamer **1B**) both the HOMO and HOMO-3 orbitals are symmetric combinations of the silole  $\pi$  orbital and both P lone pairs, while the HOMO-1 is the anti-combination of the two P lone pairs. The different interactions result in some changes in the orbital energies between the different rotamers ( $\epsilon=-7.39$  and  $-7.47$  eV, – see **Figure 3**). Altogether, the HOMO–LUMO gap of **1** depends somewhat on the actual rotamer, but in any case decreases significantly compared to the model compound **M**.

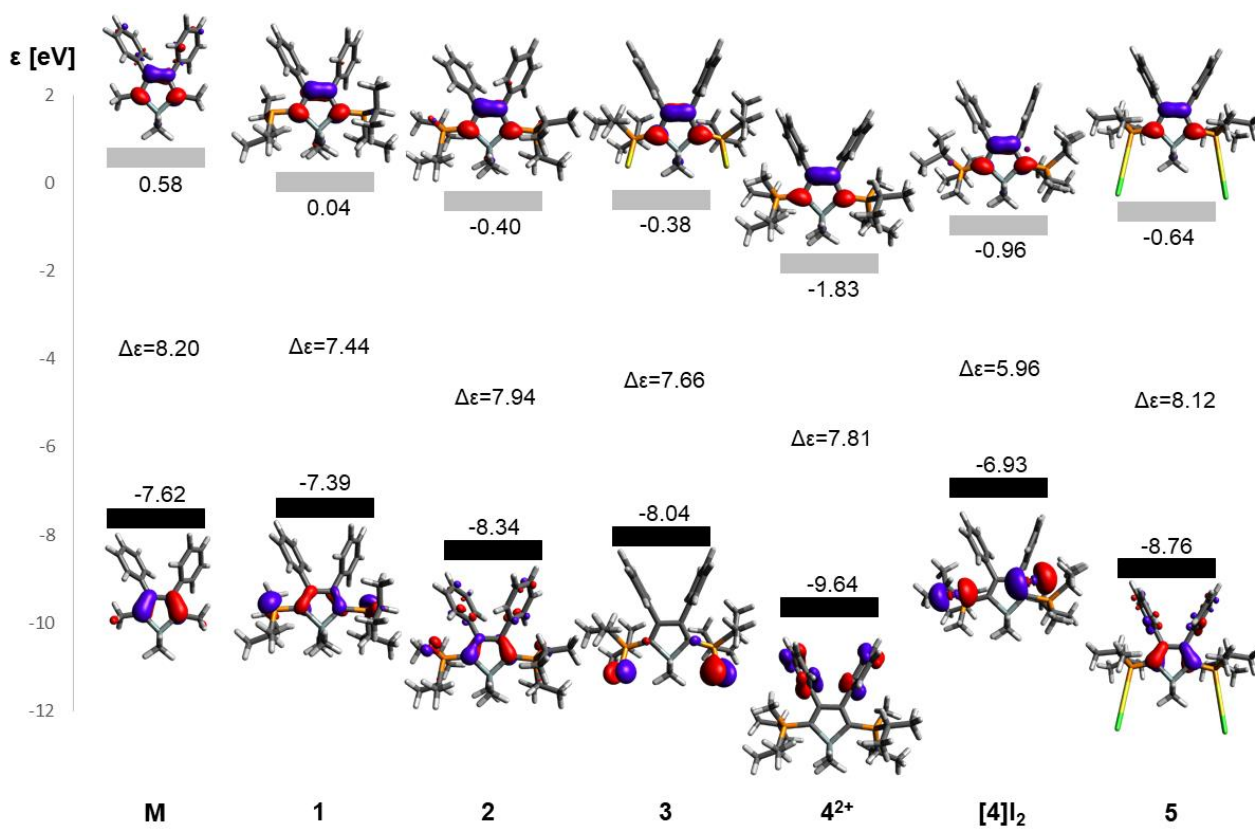


**Figure 2.** Selected orbitals of siloles **M** and **1–5** and their energies in eV at the  $\omega$ B97XD/cc-pVDZ(PCM) level and  $\omega$ B97XD/cc-pVDZ(-PP)(PCM) level for the gold complex **5** (contour value: 0.06), for **1** only the  $C_2$  symmetric rotamer is presented

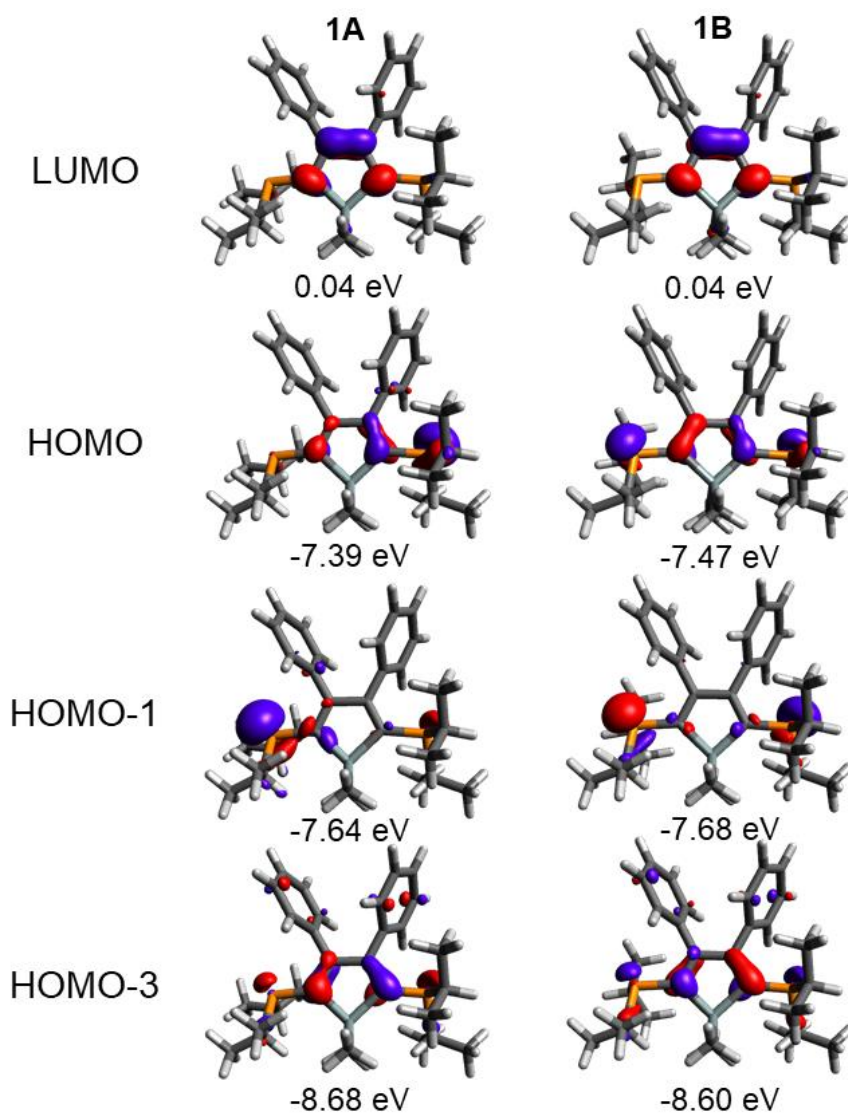


**Figure 3.** LUMO, HOMO, HOMO-1 and HOMO-3 orbitals and their energies for rotamer **1A** and **1B** at the  $\omega$ B97XD/cc-pVDZ(PCM) level. The relative energy of **1B** is 0.7 kcal/mol compared to that of **1A**.

The oxidation of **1** to **2**, as usual, results in the stabilization of both the HOMO and LUMO levels (**Table 2**). In the case of compound **2** the lone pairs at the oxygen atoms contribute only moderately to the HOMO, since the lone pairs of the oxygen are distant from the  $\pi$ -system, furthermore, they lie at much lower energy than those of the phosphorus in **1**. Hence, the HOMO energy of **2** is significantly lower ( $\epsilon = -8.34$  eV) than for **1**, but the energy of the LUMO ( $\pi^*$  type) is just slightly lower than that of **1** ( $\epsilon = -0.40$  eV). Therefore, the HOMO-LUMO gap for

**2** ( $\epsilon=-7.94$  eV) is larger than in case of **1**. In contrast, the HOMO of silole **3** is practically formed from the sulfur lone pairs, which lie higher in energy compared to those of oxygen, therefore the HOMO has higher energy ( $\epsilon=-8.04$  eV) compared to **2**. The LUMO is again a  $\pi^*$  orbital with nearly the same energy ( $\epsilon=-0.38$  eV) as for compound **2**, so the HOMO-LUMO gap becomes smaller (7.66 eV) than for silole **2**. In the case of phosphonium dication [**4**]<sup>2+</sup>, the LUMO is the silole  $\pi^*$  orbital, however, the HOMO is located exclusively at the phenyl rings (the silole  $\pi$  orbital is HOMO-4 at  $\epsilon=-10.30$  eV). Due to the (di)cationic nature, both HOMO and LUMO are significantly stabilized with respect to the orbitals of the neutral species. Besides this the neutral contact ion pair [**4**]**I**<sub>2</sub> has also been calculated, for which the LUMO is again a  $\pi^*$  orbital localized on the silole core, however, the uppermost orbitals are combinations of the iodide counter ion lone pairs. These orbitals of [**4**]**I**<sub>2</sub> are at significantly higher energy than that of [**4**]<sup>2+</sup>, but altogether the LUMO of the contact ion pair is still the most stabilized among the neutral systems. In the gold complex (no free phosphorus lone pair is available) the HOMO is located at the silole core with minor involvement of the phenyl groups. Both HOMO ( $\epsilon=-8.76$  eV) and LUMO ( $\epsilon=-0.64$  eV) are stabilized with respect to the corresponding orbitals of **1**.

**Table 2.** Electrochemical data<sup>a</sup> obtained by cyclic voltammetry and energies of the HOMO and LUMO orbitals (at the  $\omega$ B97XD/cc-pVDZ(PCM) level and  $\omega$ B97XD/cc-pVDZ(-PP)(PCM) level) for compounds **1–5** and the model compound (**M**).

	$E_{\text{ox}}$ [V] <sup>a</sup>	$E_{\text{red}}$ [V] <sup>a</sup>	$\epsilon(\text{HOMO})$ [eV]	$\epsilon(\text{LUMO})$ [eV]
<b>1</b>	+0.62 <sup>b</sup>	–	–7.39	0.04
<b>2</b>	+1.14	–2.19 <sup>b</sup>	–8.34	–0.40
<b>3</b>	+0.94	–2.12 <sup>b</sup>	–8.04	–0.38
[ <b>4</b> ] <b>I</b> <sub>2</sub>	–	–1.06 <sup>b</sup>	–6.93	–0.96
<b>5</b>	–	–1.84	–8.76	–0.64
<b>M</b>	–	–	–7.62	0.58

<sup>a</sup> In CH<sub>2</sub>Cl<sub>2</sub> with Bu<sub>4</sub>N<sup>+</sup>PF<sub>6</sub><sup>–</sup> (0.2M) at scan rate of 100 mVs<sup>–1</sup>,  $E^{\text{ox}}$  ( $E^{\text{red}}$ ) = 1/2 ( $E_{\text{pc}}$  +  $E_{\text{pa}}$ ) for reversible or quasi-reversible processes, otherwise  $E^{\text{ox}}$  ( $E^{\text{red}}$ ) = ( $E_{\text{pa}}$ ). Potentials referred vs. the ferrocene/ferrocenium couple, <sup>b</sup> quasi-reversible processes.

The redox data obtained from cyclic voltammetry (in CH<sub>2</sub>Cl<sub>2</sub> with Bu<sub>4</sub>N<sup>+</sup>PF<sub>6</sub><sup>-</sup> (0.2M) at scan rate of 100 mVs<sup>-1</sup>, **Table 2**) nicely agrees with the trends in the HOMO and LUMO energies. For compounds **[4]I<sub>2</sub>** and **5** no oxidation, while for **1** no reduction has been observed in the experimental window of -2.2 to 1.5 V vs. SCE. The oxidation potentials increase in the order of **1**<**3**<**2**, in agreement with the decreasing HOMO energies in this series. The most negative reduction potentials are observed for species **2** and **3**, and accordingly the LUMO of these two siloles lie at similar and rather low energies. Compared to these compounds, the dication **[4]I<sub>2</sub>** can be reduced at the least negative potential (-1.06 V vs. Fc/Fc<sup>+</sup>), which corresponds to its highly stabilized LUMO (see above). This compound appears as a good electron acceptor, as usually observed for phosphonium derivatives<sup>[19]</sup>. The digold complex **5** occupies an intermediate reduction potential between those of **2**, **3** and **[4]I<sub>2</sub>**, in a nice agreement with its moderately stabilized LUMO energy compared to **2** and **3**.

### Optical properties and TD-DFT calculations

The electronic absorption data of compounds **1–5** are summarized in **Table 3**, **Figure 4**. The UV-vis absorption band maxima corresponding to the lowest energy excitation of the compounds is located between 290 and 340 nm, while for **1** and **[4]I<sub>2</sub>** an additional long tailing feature could be found in the spectrum.

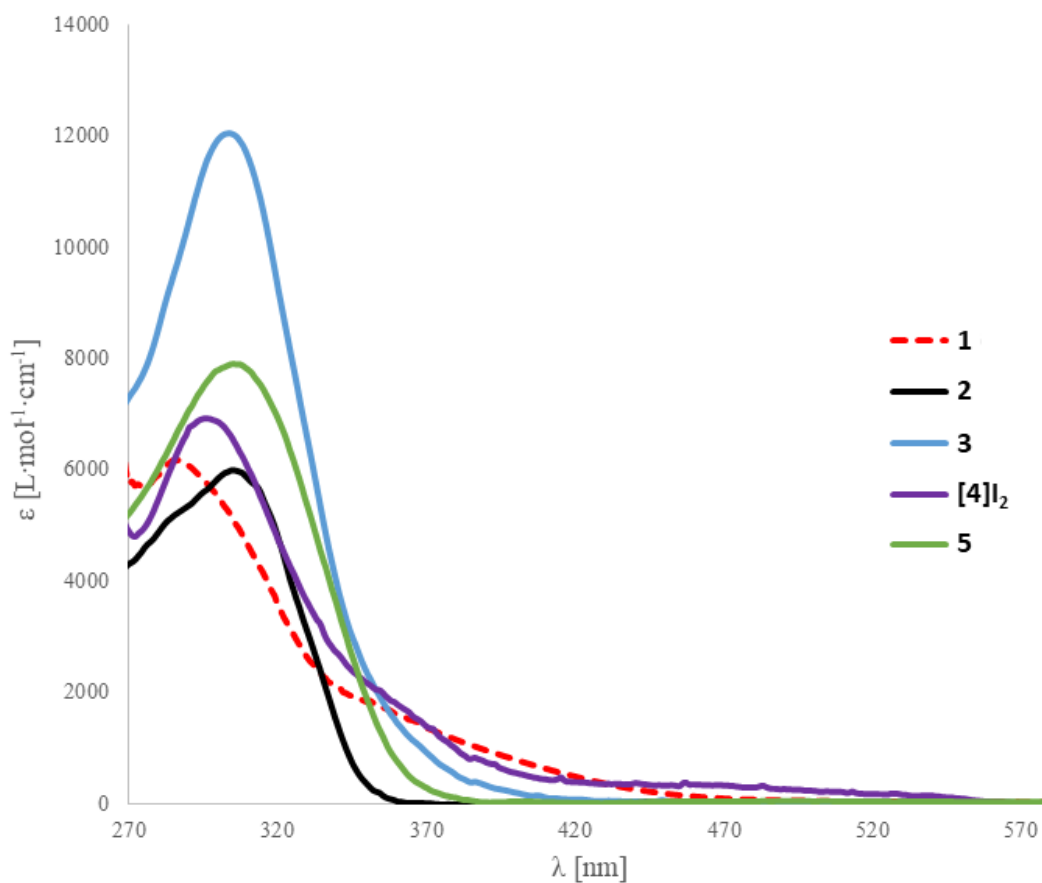


**Figure 4.** UV-vis spectra of the siloles **1–5** in dichloromethane ( $c=10^{-5}$  M). The curve for compound **1** is shown with dashed line as a possible oxidation of the compound (in the region 270 to 320 nm) cannot be excluded.

**Table 3.** Experimental and calculated optical data of siloles **1–5**. (For further transitions in the TD-DFT simulations see Supporting Information.)

Compound	Measured $\lambda_{\max}$ <sup>a</sup> [nm]	$\lambda_{\text{onset}}$ <sup>a</sup> [nm]	Calculated $\lambda_{\max}$ <sup>b</sup> [nm]	Contribution of transitions <sup>b</sup> [%]
<b>1</b>	–	470	347 <sup>c</sup> (0.1591) <sup>c</sup>	94 <sup>c</sup> (HOMO→LUMO)
<b>2</b>	312	348	305 (0.1228)	86 (HOMO→LUMO)
<b>3</b>	307	361	306 (0.1844)	53 (HOMO→LUMO) 22 (HOMO-4→LUMO)
<b>[4]<sup>2+</sup></b>	–	–	299 (0.0456)	92 (HOMO→LUMO)
			293 (0.2279)	35 (HOMO-4→LUMO)
				58 (HOMO-2→LUMO)
<b>[4]I<sub>2</sub></b>	289	404	412 (0.0046)	36 (HOMO→LUMO)
				56 (HOMO-1→LUMO)
			287 (0.1583)	66 (HOMO-8→LUMO)
<b>5</b>	308	366	301 (0.2547)	83 (HOMO→LUMO)

<sup>a</sup>: In CH<sub>2</sub>Cl<sub>2</sub> (10<sup>-5</sup> M) <sup>b</sup>: At the  $\omega$ B97XD/cc-pVDZ(PCM) level for **1-4** and  $\omega$ B97XD/cc-pVDZ(-PP)(PCM) level for the gold complex **5**, oscillator strengths are shown in parenthesis <sup>c</sup>: calculated for the rotamer with C<sub>2</sub> symmetry

To gain more insight into the optical properties, TD-DFT calculations were carried out at different levels of theory to describe the vertical excitation energies (for details see **Table S7** in the Supporting Information). Also we considered solvent effects using polarizable continuum

solvent model (PCM) with dichloromethane as solvent. In the following only the results obtained at the  $\omega$ B97XD/cc-pVDZ(PCM) level (and at the  $\omega$ B97XD/cc-pVDZ(-PP)(PCM) level for the gold complex **5**) are discussed as they offer the best agreement with the experiments.

The measured and calculated UV-Vis absorption bands agree nicely for **2**, **3** and **5**, the deviation between the experimental and computed absorption maxima being less than 10 nm. For these compounds,  $S_1 \leftarrow S_0$  (largest wavelength) corresponds basically to the HOMO  $\rightarrow$  LUMO transition (in case of **3** also the HOMO-4  $\rightarrow$  LUMO excitation has a non-negligible contribution (**Table 3**). For these compounds the first excitation is accompanied with some further excitation processes of reduced intensity, which are close in energy (see **Tables S6, S7, S13-S15, S17** in the Supporting Information). Apparently, the measured spectra are in clear accordance with these calculated results.

In case of silole **1**, the long wavelength tail of the spectrum is responsible for the yellow color. According to the  $\omega$ B97XD/cc-pVDZ TD-DFT calculations two absorptions can be attributed to excitations from the P(III) lone pair into the silole  $\pi^*$  orbitals. The numerical agreement between the calculated vertical excitation energies and the spectral position of the tailing part of the spectrum is acceptable (and is even somewhat better with the B3LYP functional), and considering that several rotamers can contribute to the spectrum with somewhat different band positions (for the calculated values see Table S6 in the Supporting Information) the broadness of this spectral feature is understandable. Nevertheless, the calculated oscillator strength would indicate more intensity in this low energy region. However, the maximum at 285 nm was not reproduced by the computations, which predict only low-intensity absorptions in this region. This disagreement is unexpected since the calculations provided a good description for the other derivatives as was discussed above. Apparently, this discrepancy may arise due to the approximate nature of the computational method. On the other hand, however, the oxidation of

compound **1** cannot be excluded despite the careful handling of the investigated solution during the measurement, which may result in absorption in the range of 270-320 nm (see above). Repeating the measurements of the UV spectra several times, we observed changes in the relative intensity in the 280 nm region, but we were able to reproduce the spectra shown in Figure 4, and in no case was the relative intensity of this spectral region lower than shown in this Figure. Altogether, while the yellow color of **1** could be fully understood, the higher energy part of the spectrum of **1** should be considered with sore reservation.

In case of **[4]I<sub>2</sub>** the position of the band maximum ( $\lambda_{\text{exp}}=289$  nm) is well described by calculating the isolated dication ( $\lambda_{\text{calc}}=299$  nm and 293 nm) or the contact ion pair **[4]I<sub>2</sub>** ( $\lambda_{\text{calc}}=287$  nm). Furthermore, the position of the low intensity shoulder ( $\lambda_{\text{onset}}=404$  nm) is in agreement with the calculated first six excitations of **[4]I<sub>2</sub>** in the range of  $\lambda_{\text{calc}}=337$  to 412 nm with low intensities (see **Table S18** in Supporting Information), which belong to charge transfer excitations from the iodide ions to the silole LUMO.

## Conclusion

We have presented the synthesis of bisphosphanil siloles bearing versatile functionalization at the P centers. These new compounds have been fully characterized by multinuclear NMR spectroscopy, HRMS, elemental analysis and X-ray crystallography. Besides the synthesis, the impact of the modification at the phosphanyl substituent was studied experimentally, with UV-vis absorption spectroscopy and cyclic voltammetry as well as theoretically using TD-DFT calculations. It has been shown that the 2,5-bisphosphanilsilole can be used as a precursor in different types of reactions (eg. oxidation, sulfurization or complexation) and the optical and electrochemical properties of these compounds are influenced by the derivatization of the phosphorus center. With the theoretical calculations the modifications on the phosphanyl substituents were studied to understand the electronic effects of the changes, which were not

studied earlier by TD-DFT calculations. This structure-property relationship study provides a better understanding of the electronic properties of these systems, and thus paves the way toward their further incorporation into optoelectronic devices.

## Experimental section

**General:** All reactions were performed in oven-dried glassware under argon or nitrogen atmosphere using standard Schlenk techniques. Solvents were dried according to well-known procedures (THF, diethyl ether and C<sub>6</sub>D<sub>6</sub> over sodium/benzophenone, hexane over LiAlH<sub>4</sub>, dichloromethane over P<sub>2</sub>O<sub>5</sub>) and distilled or condensed freshly before use. Solids were dried in vacuum. Chlorotriphenylsilane<sup>[41]</sup> and chlorodiisopropylphosphine<sup>[42]</sup> were synthesized following literature descriptions.

NMR spectra were recorded on a Bruker AM300, a Bruker Avance 300, a Bruker Avance III HD 500 MHz, or a Bruker DRX-500 spectrometers (using the deuterated solvent as internal lock and TMS (for <sup>1</sup>H, <sup>13</sup>C and <sup>29</sup>Si) and 85% aqueous H<sub>3</sub>PO<sub>4</sub> (for <sup>31</sup>P) as external standards, chemical shifts given in ppm). DEPT, HMBC and HSQC measurements were carried out to help to interpret the peaks of the silole and phenyl rings. The UV-Vis spectra were recorded on Perkin Elmer Lambda 25 UV-vis spectrometer. High resolution mass spectra were recorded with Micromass GCT (70 eV; DIR-EI) and Agilent LC-MS 6510. The elemental analysis were performed with Elementar vario MICRO cube and with the apparatus of the CRMPO in University of Rennes 1.

The single crystal of **1**, **2** and **3** were mounted on a loop. Intensity data were collected on a R-AXIS-RAPID diffractometer (monochromator; Mo-K $\alpha$  radiation,  $\lambda = 0.71073$  Å) at 103(2) K. The single crystal of **5** was mounted on a loop and the intensity data were collected on a D8 VENTURE Bruker AXS diffractometer (monochromator: Mo-K $\alpha$  radiation,  $\lambda = 0.71073$  Å), at 150(2) K. Crystal Clear<sup>[43]</sup> (developed by Rigaku Company) software was used for data

collection and refinement in the cases of **1**, **2** and **3**. Numerical absorption corrections or empirical correction<sup>[44,45]</sup>, were applied to the data. The structures were solved by direct methods. Anisotropic full-matrix least-squares refinements were performed on  $F^2$  for all non-hydrogen atoms. Hydrogen atoms bonded to C atoms were placed in calculated positions and refined in a riding-model approximation. The computer programs used for the structure solution, refinement and analysis of the structures were Shelx<sup>[46,47]</sup>, Sir2014<sup>[48]</sup>, Wingx<sup>[49]</sup> and Platon<sup>[50]</sup>. The solid state structure of **5** contains disordered dichloromethane molecules, which were also modelled. Program Mercury<sup>[31]</sup> was used for the graphical representation. Details of crystallographic data, data collection and refinement for crystal **1**, **2**, **3** and **5** are collected in **Table S1-S3**. CCDC 1977534-1977536, 1978863 contains the supplementary crystallographic data for this paper. These data can be obtained free of charge from The Cambridge Crystallographic Data Centre *via* [www.ccdc.cam.ac.uk/structures](http://www.ccdc.cam.ac.uk/structures).

**Synthesis of 1:** The synthesis of **1** was carried out following modified Tamao's method<sup>[51]</sup>. 3.60 g (27.3 mmol) naphthalene and 0.192 g (27.3 mmol) lithium were stirred in 70 mL THF under argon at room temperature until the solid lithium pieces disappeared. The mixture was cooled to  $-60^{\circ}\text{C}$  and 1.773 g (6.817 mmol) dimethyl-bis(phenylethynyl)silane was added dropwise and the mixture was stirred for an hour at  $-60^{\circ}\text{C}$ . Then the solution of 4.15 g (13.63 mmol) chlorotriphenylsilane with 20 ml THF was added dropwise and after 20 minutes stirring at  $-60^{\circ}\text{C}$  2.2 mL (13.63 mmol) chlorodiisopropylphosphine was added dropwise. Then the mixture was allowed to warm to room temperature and it was stirred for a day. The solvent was removed under reduced pressure and after the addition of dry hexane the insoluble lithium salt was filtered and the solvent was removed under reduced pressure. Naphthalene was removed by sublimation (at  $100^{\circ}\text{C}/0.1$  mbar) and the yellow product was crystallized from diethyl ether at  $-35^{\circ}\text{C}$  yielding **1**. (2.53 g, 75%). <sup>1</sup>H NMR (300.1 MHz, C<sub>6</sub>D<sub>6</sub>):  $\delta$  = 0.59 (s, 6H, SiCH<sub>3</sub>); 1.07 (m, 24H, CHCH<sub>3</sub>); 2.00 (m, 4H, CH); 6.80–6.90 (m, 2H, *p*ArH), 6.92–7.02 (m,

8H, *o/mArH*).  $^{13}\text{C}$   $\{^1\text{H}\}$  NMR (75.5 MHz,  $\text{C}_6\text{D}_6$ ):  $\delta$  = 0.1 (s,  $\text{SiCH}_3$ ); 21.9 (d,  $^2J_{\text{C,P}} = 21.7$  Hz,  $\text{CCH}_3$ ); 22.6 (d,  $^2J_{\text{C,P}} = 15.1$  Hz,  $\text{CCH}_3$ ); 26.4 (d,  $^1J_{\text{C,P}} = 13.6$ ,  $\text{CCH}_3$  Hz); 126.4 (*pPh*); 127.2 (*mPh*); 130.5 (d,  $^4J_{\text{C,P}} = 2.9$  Hz, *oPh*); 141.2 (d,  $^3J_{\text{C,P}} = 7.1$  Hz, *iPh*); 143.1 (dd  $^1J_{\text{C,P}} = 27.9$  Hz,  $^3J_{\text{C,P}} = 2.2$  Hz,  $\text{C}_\alpha$ ); 170.5 (dd,  $^2J_{\text{C,P}} = 25.7$  Hz,  $^3J_{\text{C,P}} = 5.8$  Hz,  $\text{C}_\beta$ ).  $^{29}\text{Si}\{^1\text{H}\}$  NMR (99.4 MHz,  $\text{C}_6\text{D}_6$ ):  $\delta$  = 12.6 (t,  $^2J_{\text{P,Si}} = 8.5$  Hz).  $^{31}\text{P}\{^1\text{H}\}$  NMR (121.5 MHz,  $\text{C}_6\text{D}_6$ ):  $\delta$  = 8.6 (s). HR-MS (EI,  $m/z$ )  $[\text{M}]^+$  calcd for  $\text{C}_{30}\text{H}_{44}\text{P}_2\text{Si}$ : 494.2670; found: 494.2688. Anal. Calcd. for  $\text{C}_{30}\text{H}_{44}\text{P}_2\text{Si}$  : C, 72.84, H, 8.96; Found: C, 71.75, H, 8.12. Melting point: 144-146 °C.

**Synthesis of 2:** At room temperature to a solution of 0.131 g (0.265 mmol) **1** in 10 mL dichloromethane 0.2 mL 30 % aqueous solution hydrogen peroxide was added dropwise and it was stirred for 3 hours. Then 10 mL 5 % sodium thiosulfate was added and then the water phase was extracted with dichloromethane. The combined organic layer was dried with anhydrous  $\text{MgSO}_4$  and the solvent was evaporated then the product was isolated as a white powder (0.106 g, 76%).  $^1\text{H}$  NMR (500.1 MHz,  $\text{CDCl}_3$ ):  $\delta$  = 0.64 (s, 6H,  $\text{SiCH}_3$ ); 0.9–1.1 (m, 24H,  $\text{CHCH}_3$ ); 1.3–1.4 (m, 4H, CH); 6.7–7.1 (m, 10H, ArH).  $^{13}\text{C}\{^1\text{H}\}$  NMR (125.8 MHz,  $\text{CDCl}_3$ ):  $\delta$  = –4.0; 15.1 (d,  $^2J_{\text{C,P}} = 3.4$  Hz); 16.3 (d,  $^2J_{\text{C,P}} = 2.2$  Hz); 27.8 (d,  $^1J_{\text{C,P}} = 65.0$  Hz); 126.5; 126.6; 126.8; 138.3 (d,  $^2J_{\text{C,P}} = 5.1$  Hz); 144.9 (dd,  $^1J_{\text{C,P}} = 71.2$  Hz,  $^3J_{\text{C,P}} = 3.8$  Hz); 160.6 (d,  $J_{\text{C,P}} = 18.5$  Hz).  $^{29}\text{Si}\{^1\text{H}\}$  NMR (99.4 MHz,  $\text{CDCl}_3$ ):  $\delta$  = 23.1 (t,  $^2J_{\text{P,Si}} = 10.5$  Hz, Si-ring).  $^{31}\text{P}\{^1\text{H}\}$  NMR (121.5 MHz,  $\text{CDCl}_3$ ):  $\delta$  = 52.1 (s). HR-MS (ESI,  $\text{CH}_2\text{Cl}_2/\text{CH}_3\text{OH}$ : 60/40,  $m/z$ )  $[\text{M}+\text{H}]^+$  calcd for  $\text{C}_{30}\text{H}_{45}\text{O}_2\text{P}_2\text{Si}$ : 527.2659, found: 527.2667. Anal. Calcd. for  $\text{C}_{30}\text{H}_{44}\text{O}_2\text{P}_2\text{Si}$  : C, 68.41, H, 8.42; Found: C, 66.32, H, 8.24. Melting point: 254-256 °C.

**Synthesis of 3:** To a solution of 0.097 g (1.963 mmol) of **1** in 20 mL diethyl ether 0.32 g (10.0 mmol) sulfur was added then the mixture was stirred for 30 minutes at room temperature. Then the solvent was evaporated and the crude mixture was purified by silica gel chromatography (eluent hexane/dichloromethane 100/0→50/50) to afford **3** as a white powder. (0.089 g, 81 %)

**<sup>1</sup>H NMR** (300.1 MHz, CDCl<sub>3</sub>): δ = 0.90 (s, 6H, SiCH<sub>3</sub>); 1.01 (dd, <sup>3</sup>J<sub>H,P</sub> = 17.7 Hz, <sup>3</sup>J<sub>H,H</sub> = 6.6 Hz, 24H, CHCH<sub>3</sub>); 1.12 (dd, <sup>3</sup>J<sub>H,P</sub> = 17.7 Hz, <sup>3</sup>J<sub>H,H</sub> = 6.9 Hz, 12H, CHCH<sub>3</sub>); 1.69 (m, 4H, CH); 6.8–7.2 (m, 10H, ArH). **<sup>13</sup>C{<sup>1</sup>H} NMR** (75.5 MHz, CDCl<sub>3</sub>): δ = 0.5; 17.1; 18.6; 30.3 (d, <sup>1</sup>J<sub>C,P</sub> = 47.1 Hz); 127.7; 127.7; 127.8; 138.9 (d, J<sub>C,P</sub> = 6.2 Hz); 143.6 (dd, <sup>1</sup>J<sub>C,P</sub> = 49.0 Hz, <sup>3</sup>J<sub>C,P</sub> = 1.9 Hz); 161.4 (dd, <sup>2</sup>J<sub>C,P</sub> = 19.2 Hz, <sup>3</sup>J<sub>C,P</sub> = 1.2 Hz). **<sup>29</sup>Si{<sup>1</sup>H} NMR** (99.4 MHz, CDCl<sub>3</sub>): δ = 22.4 (d, <sup>2</sup>J<sub>P,Si</sub> = 15.7 Hz, Si-ring). **<sup>31</sup>P {<sup>1</sup>H} NMR** (121.5 MHz, CDCl<sub>3</sub>): δ = 63.5 (s). HR-MS (ESI, CH<sub>2</sub>Cl<sub>2</sub>/ CH<sub>3</sub>OH: 60/40, m/z) [M+H]<sup>+</sup> calcd for C<sub>30</sub>H<sub>45</sub>P<sub>2</sub>S<sub>2</sub>Si: 559.2202, found: 559.2194. Anal. Calcd. for C<sub>30</sub>H<sub>44</sub>P<sub>2</sub>S<sub>2</sub>Si : C, 64.48, H, 7.94, S, 11.48; Found: C, 64.42, H, 7.60, S, 11.36. Melting point: 265-267 °C.

**Synthesis of [4]I<sub>2</sub>**: To a solution of 0.119 g (0.241 mmol) **1** in 30 mL diethyl ether 0.53 mL (8.51 mmol) methyl iodide was added dropwise at room temperature, then the mixture was stirred for a day. During the reaction the product was precipitated as a yellow solid. **[4]I<sub>2</sub>** was filtered and washed with diethyl ether yielding **[4]I<sub>2</sub>** (0.154 g, 82 %).

**<sup>1</sup>H NMR** (300.1 MHz, CDCl<sub>3</sub>): δ = 1.19 (s, 6H, SiCH<sub>3</sub>); 1.30 (dd, <sup>3</sup>J<sub>H,P</sub> = 17.9 Hz, <sup>3</sup>J<sub>H,H</sub> = 6.9 Hz, 12H, CHCH<sub>3</sub>); 1.40 (dd, <sup>3</sup>J<sub>H,P</sub> = 18.2 Hz, <sup>3</sup>J<sub>H,H</sub> = 7.2 Hz, 12H, CHCH<sub>3</sub>); 1.68 (d, <sup>2</sup>J<sub>H,P</sub> = 12.0 Hz, 6H, PCH<sub>3</sub>); 2.70 (m, 4H, CH); 7.1–7.2 (m, 6H, ArH); 7.4–7.6 (m, 4H, ArH).

**<sup>13</sup>C{<sup>1</sup>H} NMR** (75.5 MHz, CDCl<sub>3</sub>): δ = 1.1; 2.5 (d, <sup>1</sup>J<sub>C,P</sub> = 52.2 Hz); 17.4; 18.9; 25.7 (d, <sup>1</sup>J<sub>C,P</sub> = 45.6 Hz); 128.1; 129.0; 129.4; 136.4 (d, J<sub>C,P</sub> = 7.4 Hz); the C peaks of the silole ring do not appear in the spectrum, due to the low solubility of the compound. **<sup>29</sup>Si{<sup>1</sup>H} NMR** (99.4 MHz, CDCl<sub>3</sub>): δ = 24.0 (t, <sup>2</sup>J<sub>P,Si</sub> = 18.7 Hz, Si-ring). **<sup>31</sup>P {<sup>1</sup>H} NMR** (121.5 MHz, CDCl<sub>3</sub>): δ = 38.4 (s). HR-MS (EI, m/z) [M<sub>3</sub>]<sup>+</sup> calcd for C<sub>31</sub>H<sub>47</sub>P<sub>2</sub>Si: 509.2917; found: 509.2904. Anal. Calcd. for C<sub>32</sub>H<sub>50</sub>I<sub>2</sub>P<sub>2</sub>Si : C, 49.37, H, 6.47; Found: C, 43.62.81, H, 6.59. The low carbon value is most likely due to the formation of uncombustable carbon particles.

**Synthesis of 5**: To a solution of 0.020 g (0.04 mmol) of **1** in 5 mL dichloromethane 0.027 g (0.081 mmol) chloro(tetrahydrothiophene)gold(I) was added and the mixture was stirred for 10

minutes at room temperature. Then the solvent was evaporated under reduced pressure and the crude was washed with toluene. The product was crystallized from dichloromethane-pentane mixture with slow evaporation at room temperature yielding **5** (0.035g, 90%).

**<sup>1</sup>H NMR** (400.2 MHz, CD<sub>2</sub>Cl<sub>2</sub>): δ = 0.94 (s, 6H, SiCH<sub>3</sub>); 1.13-1.29 (m, 24H, CHCH<sub>3</sub>); 2.00-2.18 (m 4H, CH); 6.81-7.25 (m, 10H, ArH). **<sup>13</sup>C{<sup>1</sup>H} NMR** (100.6 MHz, CD<sub>2</sub>Cl<sub>2</sub>): δ = -1.4; 21.6 (d, <sup>2</sup>J<sub>C,P</sub> = 2.1 Hz); 21.8 (d, <sup>2</sup>J<sub>C,P</sub> = 5.6 Hz); 28.4 (<sup>1</sup>J<sub>C,P</sub> = 34.5 Hz); 128.5; 135.8 (d, <sup>2</sup>J<sub>C,P</sub> = 1.7 Hz); 136.1; 138.6 (d, <sup>2</sup>J<sub>C,P</sub> = 7.7 Hz); 170.7 (d, J<sub>C,P</sub> = 14.6 Hz). **<sup>29</sup>Si{<sup>1</sup>H} NMR** (79.5 MHz, CD<sub>2</sub>Cl<sub>2</sub>): δ = 18.3 (t, <sup>2</sup>J<sub>Si,P</sub> = 17.6 Hz, Si-ring). **<sup>31</sup>P {<sup>1</sup>H} NMR** (162.0 MHz, CD<sub>2</sub>Cl<sub>2</sub>): δ = 47.1 (s). HR-MS (ESI, CH<sub>2</sub>Cl<sub>2</sub>/CH<sub>3</sub>OH: 80/20, m/z) [M+Na]<sup>+</sup> calcd for C<sub>30</sub>H<sub>44</sub><sup>35</sup>Cl<sub>2</sub>NaSiP<sub>2</sub>Au<sub>2</sub>: 981.1288, found: 981.1285.

**Theoretical calculations:** The computations were carried out with the Gaussian 09 suite of programs<sup>[52]</sup>. All structures were optimized using the B3LYP and ωB97XD functionals combined with the 6-31+G\*, 6-31G\*, def2svp (for gold), cc-pVDZ, and cc-pVDZ(-pp) (for gold and iodine) basis sets. In the polarized continuum model (PCM) the solvent was dichloromethane. At each of the optimized structures vibrational analysis was performed to check that the stationary point located is a minimum on the potential energy hypersurface (no imaginary frequencies were obtained). In the TD-DFT calculations the first 20 excitations were considered. The molecular orbitals were plotted with Avogadro program<sup>[53]</sup>. The geometries were visualized with Molden<sup>[54,55]</sup>.

## Acknowledgement

We would like to thank for the support of the Ministère de la Recherche et de l'Enseignement Supérieur, the CNRS, the Région Bretagne, Campus France, the French National Research Agency (ANR Heterographene ANR-16-CE05-0003-01), NKFIH NN 113772, PD 116329, PD 128504 Varga József Alapítvány, Pro Progressio Alapítvány, Tempus Közalapítvány, János Bolyai Research Fellowship (for H. T. and Z. B.), ÚNKP-19-4-BME-422, TÉT\_16-1- 2016-

0128 BME-Nanonotechnology FIKP grant of EMMI (BME FIKP-NAT), PICS SmartPAH (08062), China-French AIL in “Functional Organophosphorus Materials”, GDR Phosphore.

## References:

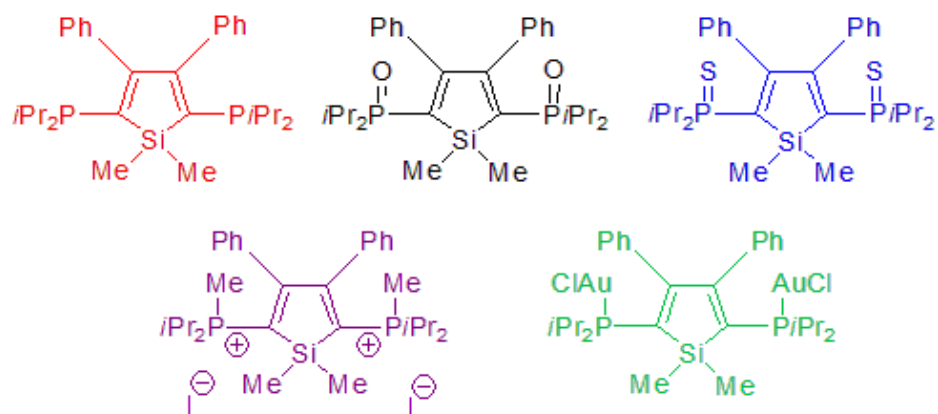
- [1] J. Roncali, *Chem. Rev.* **1997**, *97*, 173–205.
- [2] M. Hissler, P. W. Dyer, R. Réau, *Coord. Chem. Rev.* **2003**, *244*, 1–44.
- [3] S. Yamaguchi, K. Tamao, *J. Chem. Soc., Dalt. Trans.* **1998**, 3693–3702.
- [4] Y. Shirota, H. Kageyama, *Chem. Rev.* **2007**, *107*, 953–1010.
- [5] K. Tamao, M. Uchida, T. Izumizawa, K. Furukawa, S. Yamaguchi, *J. Am. Chem. Soc.* **1996**, *118*, 11974–11975.
- [6] M. Wong, Y. L. Ho, D. B. Zhu, H. Y. Chen, W. Y. Lam, B. Z. Tang, J. D. Luo, H. S. Kwok, *Appl. Phys. Lett.* **2002**, *81*, 574–576.
- [7] J. Lee, Q. De Liu, D. R. Bai, Y. Kang, Y. Tao, S. Wang, *Organometallics* **2004**, *23*, 6205–6213.
- [8] H. Usta, G. Lu, A. Facchetti, T. J. Marks, *J. Am. Chem. Soc.* **2006**, *128*, 9034–9035.
- [9] G. Lu, H. Usta, C. Risko, L. Wang, A. Facchetti, M. A. Ratner, T. J. Marks, *J. Am. Chem. Soc.* **2008**, *130*, 7670–7685.
- [10] Y. Cai, A. Qin, B. Z. Tang, *J. Mater. Chem. C* **2017**, *5*, 7375–7389.
- [11] J. Luo, Z. Xie, J. W. Y. Lam, L. Cheng, B. Z. Tang, H. Chen, C. Qiu, H. S. Kwok, X. Zhan, Y. Liu, et al., *Chem. Commun.* **2001**, *18*, 1740–1741; H. Sohn, R. R. Huddleston, D. R. Powell, R. West, K. Oka, X. Yonghua, *J. Am. Chem. Soc.* **1999**, *121*, 2935–2936. H. Chen, M. Denis, P.-A. Bouit, Y. Zhang, X. Wei, D. Tondelier, B. Geffroy, Z. Duan, M. Hissler *Appl. Sci.* **2018**, *8*(5), 812–822
- [12] R. T. K. Kwok, C. W. T. Leung, J. W. Y. Lam, B. Z. Tang, *Chem. Soc. Rev.* **2015**, *44*, 4228–4238.
- [14] S. Yamaguchi, R. Jin, S. Ohno, K. Tamao, *Organometallics* **1998**, *17*, 5133–5138.
- [15] H. J. Son, W. S. Han, J. Y. Chun, S. N. Kwon, J. Ko, S. O. Kang, *Organometallics* **2008**, *27*, 2464–2473.
- [16] J. Ohshita, Y. Kurushima, K. Lee, A. Kunai, Y. Ooyama, *Organometallics* **2007**, *26*, 6591–6595.
- [17] J. Lee, Q. Liu, M. Motala, J. Dane, J. Gao, Y. Kang, S. Wang, *Chem. Mater.* **2004**, *16*, 1869–1877.
- [18] X. Zhan, S. Barlow, S. R. Marder, *Chem. Commun.* **2009**, 1948–1955.

- [19] C. Hay, M. Hissler, C. Fischmeister, J. Rault-Berthelot, L. Toupet, L. Nyulászi, R. Réau, *Chem. - A Eur. J.* **2001**, *7*, 4222–4236.
- [20] P. A. Bouit, A. Escande, R. Szücs, D. Szieberth, C. Lescop, L. Nyulászi, M. Hissler, R. Réau, *J. Am. Chem. Soc.* **2012**, *134*, 6524–6527.
- [21] H. Omori, S. Hiroto, Y. Takeda, H. Fliegl, S. Minakata, H. Shinokubo, *J. Am. Chem. Soc.* **2019**, *141*, 4800–4805.
- [22] J. Braddock-Wilking, L. Bin Gao, N. P. Rath, *Organometallics* **2010**, *29*, 1612–1621.
- [23] K. Tamao, S. Yamaguchi, *J. Am. Chem. Soc.* **1994**, *116*, 11715–11722.
- [24] J. Vicente, P. González-Herrero, Y. García-Sánchez, P. G. Jones, *Inorg. Chem.* **2009**, *48*, 2060–2071.
- [25] M. Sun, H. Y. Zhang, Q. Han, K. Yang, S. D. Yang, *Chem. - A Eur. J.* **2011**, *17*, 9566–9570.
- [26] B. Maryasin, H. Zipse, *Phys. Chem. Chem. Phys.* **2011**, *13*, 5150–5158.
- [27] E. Fluck, H. Binder, *Zeitschrift für Anorg. und Allg. Chemie* **1967**, *354*, 139–148.
- [28] D. Klintuch, K. Krekić, C. Bruhn, Z. Benkő, R. Pietschnig, *Eur. J. Inorg. Chem.* **2016**, *2016*, 718–725.
- [29] F. Roesler, B. Kaban, D. Klintuch, U. M. Ha, C. Bruhn, H. Hillmer, R. Pietschnig, *Eur. J. Inorg. Chem.* **2019**, *2019*, 4820–4825.
- [30] C. Fekete, R. Mokrai, P. Bombicz, L. Nyulászi, I. Kovács, *J. Organomet. Chem.* **2015**, *799–800*, 291–298.
- [31] C. F. Macrae, P. R. Edgington, P. McCabe, E. Pidcock, G. P. Shields, R. Taylor, M. Towler, J. van de Streek, *J. Appl. Crystallogr.* **2006**, *39*, 453–457.
- [32] J. Braddock-Wilking, Y. Zhang, J. Y. Corey, N. P. Rath, *J. Organomet. Chem.* **2008**, *693*, 1233–1242.
- [33] S. P. (Series E. Zvi Rappoport (Editor), Yitzhak Apeloig (Editor), *The Chemistry of Organic Silicon Compounds, Volume 2, Parts 1, 2, and 3 (3 Part Set)*, Wiley-VCH., **1998**.
- [34] L. Párkányi, *J. Organomet. Chem.* **1981**, *216*, 9–16.
- [35] J. J. Daly, *J. Chem. Soc.* **1964**, 3799.
- [36] J. A. Thomas, T. A. Hamor, *Acta Crystallogr. Sect. C* **1993**, *49*, 355–357.
- [37] C. Lensink, G. J. Gainsford, *Aust. J. Chem.* **1998**, *51*, 667–672.
- [38] D. Wechsler, M. A. Ranking, R. McDonald, M. J. Ferguson, G. Schatte, M. Stradiotto, *Organometallics* **2007**, *26*, 6418–6427.
- [39] N. C. Baenziger, W. E. Bennett, D. M. Soborofe, *Acta Crystallogr. Sect. B Struct.*

- Crystallogr. Cryst. Chem.* **2002**, *32*, 962–963.
- [40] M. Khan, C. Oldham, D. G. Tuck, *Can. J. Chem.* **2006**, *59*, 2714–2718.
- [41] P. J. Moehs, M. D. Gebler, T. D. Harris, *J. Inorg. Nucl. Chem.* **1981**, *43*, 235–237.
- [42] W. Voskuil, J. F. Arens, *Org. Synth.* **1968**, *48*, 47.
- [43] CrystalClear SM 1.4.0 Rigaku/MSI Inc., 2008.
- [44] NUMABS: Higashi, T. (1998), rev. 2002. (Rigaku/MSI Inc.)
- [45] R. H. Blessing, *Acta Crystallogr. Sect. A Found. Crystallogr.* **1995**, *51*, 33–38.
- [46] G. M. Sheldrick, *Acta Crystallogr. Sect. C Struct. Chem.* **2015**, *71*, 3–8.
- [47] G. M. Sheldrick, *Acta Crystallogr. Sect. A Found. Crystallogr.* **2008**, *64*, 112–122.
- [48] M. C. Burla, R. Caliandro, B. Carrozzini, G. L. Cascarano, C. Cuocci, C. Giacovazzo, M. Mallamo, A. Mazzone, G. Polidori, *J. Appl. Crystallogr.* **2015**, *48*, 306–309.
- [49] L. J. Farrugia, *J. Appl. Crystallogr.* **2012**, *45*, 849–854.
- [50] A. L. Spek, *Acta Crystallogr. Sect. D Biol. Crystallogr.* **2009**, *65*, 148–155.
- [51] S. Yamaguchi, R. Jin, K. Tamao, M. Shiro, *Organometallics* **1997**, *16*, 2230–2232.
- [52] Gaussian 09, Revision E.01, M. J. Frisch, G. W. Trucks, H. B. Schlegel, G. E. Scuseria, M. A. Robb, J. R. Cheeseman, G. Scalmani, V. Barone, B. Mennucci, G. A. Petersson, H. Nakatsuji, M. Caricato, X. Li, H. P. Hratchian, A. F. Izmaylov, J. Bloino, G. Zheng, J. L. Sonnenberg, M. Hada, M. Ehara, K. Toyota, R. Fukuda, J. Hasegawa, M. Ishida, T. Nakajima, Y. Honda, O. Kitao, H. Nakai, T. Vreven, J. A. Montgomery, Jr., J. E. Peralta, F. Ogliaro, M. Bearpark, J. J. Heyd, E. Brothers, K. N. Kudin, V. N. Staroverov, T. Keith, R. Kobayashi, J. Normand, K. Raghavachari, A. Rendell, J. C. Burant, S. S. Iyengar, J. Tomasi, M. Cossi, N. Rega, J. M. Millam, M. Klene, J. E. Knox, J. B. Cross, V. Bakken, C. Adamo, J. Jaramillo, R. Gomperts, R. E. Stratmann, O. Yazyev, A. J. Austin, R. Cammi, C. Pomelli, J. W. Ochterski, R. L. Martin, K. Morokuma, V. G. Zakrzewski, G. A. Voth, P. Salvador, J. J. Dannenberg, S. Dapprich, A. D. Daniels, O. Farkas, J. B. Foresman, J. V. Ortiz, J. Cioslowski, and D. J. Fox, Gaussian, Inc., Wallingford CT, 2013.
- [53] <https://avogadro.cc/>
- [54] G. Schaftenaar, J. H. Noordik, *J. Comput. Aided. Mol. Des.* **2000**, *14*, 123–134.
- [55] G. Schaftenaar, E. Vlieg, G. Vriend, *J. Comput. Aided. Mol. Des.* **2017**, *31*, 789–800.

Key topic: silicon heterocycles

TOC graphic:



Phosphanyl substituted siloles and their P-modified congeners have been accessed and studied by NMR spectroscopy, X-ray diffraction, UV-Vis absorption, electro chemistry and computations.